Finite-temperature ordering in a two-dimensional highly frustrated spin model

2007 J. Phys.: Condens. Matter 19 145249

(http://iopscience.iop.org/0953-8984/19/14/145249)

IOP PUBLISHING JOURNAL OF PHYSICS: CONDENSED MATTER

J. Phys.: Condens. Matter **19** (2007) 145249 (10pp) doi:10.1088/0953-8984/19/14/145249

Finite-temperature ordering in a two-dimensional highly frustrated spin model

A Honecker[1], D C Cabra[2], H-U Everts[3], P Pujol[4] and F Stauffer[2,5]

[1] Institut für Theoretische Physik, Georg-August-Universität Göttingen, Friedrich-Hund-Platz 1, 37077 Göttingen, Germany
[2] Université Louis Pasteur, Laboratoire de Physique Théorique, 67084 Strasbourg, Cédex, France
[3] Institut für Theoretische Physik, Leibniz Universität Hannover, Appelstraße 2, 30167 Hannover, Germany
[4] Laboratoire de Physique, ENS Lyon, 46 Allée d'Italie, 69364 Lyon Cédex 07, France
[5] Institut für Theoretische Physik, Universität zu Köln, Zülpicher Straße 77, 50937 Köln, Germany

E-mail: ahoneck@uni-goettingen.de

Received 13 September 2006
Published 23 March 2007
Online at stacks.iop.org/JPhysCM/19/145249

Abstract

We investigate the classical counterpart of an effective Hamiltonian for a strongly trimerized kagome lattice. Although the Hamiltonian only has a discrete symmetry, the classical groundstate manifold has a continuous global rotational symmetry. Two cases should be distinguished for the sign of the exchange constant. In one case, the groundstate has a 120° spin structure. To determine the transition temperature, we perform Monte Carlo simulations and measure the specific heat and the order parameter as well as the associated Binder cumulant. In the other case, the classical groundstates are macroscopically degenerate. A thermal order-by-disorder mechanism is predicted to select another 120° spin structure. A finite but very small transition temperature is detected by Monte Carlo simulations using the exchange method.

(Some figures in this article are in colour only in the electronic version)

1. Introduction

Highly frustrated magnets are a fascinating area of research with many challenges and surprises [1, 2]. One exotic case is the spin-1/2 Heisenberg antiferromagnet on the kagome lattice, where in particular an unusually large number of low-lying singlets have been observed numerically [3, 4]. An effective Hamiltonian approach to the strongly trimerized kagome lattice [5] was then successful in explaining the unusual properties of the homogeneous lattice [6].

Interest in this situation has been renewed recently due to the suggestion that strongly trimerized kagome lattices can be realized by fermionic quantum gases in optical lattices [7, 8].

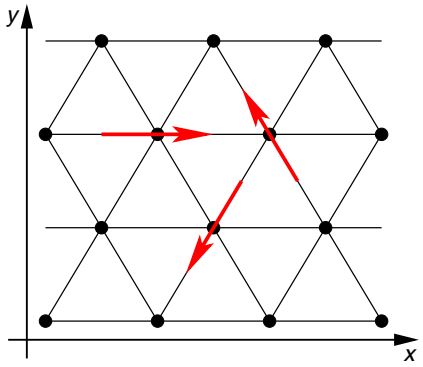

Figure 1. Part of the triangular lattice. Arrows indicate the direction of the unit vectors $\vec{e}_{i;\langle i,j\rangle}$ entering the Hamiltonian (1).

For two fermions per triangle, one obtains the aforementioned effective Hamiltonian on a triangular lattice [5], but without the original magnetic degrees of freedom. This effective Hamiltonian also describes the spin-1/2 Heisenberg antiferromagnet on the trimerized kagome lattice at one-third of the saturation magnetization [9]. Furthermore, this model shares some features with pure orbital models on the square lattice [10, 11], but it is substantially more frustrated than these models.

Numerical studies of the effective quantum Hamiltonian [12–14] provide evidence for an ordered groundstate and a possible finite-temperature ordering transition. Since the Hamiltonian only has discrete symmetries, one indeed expects a finite-temperature phase transition if the groundstate is ordered. Furthermore, quantum fluctuations should be unimportant for the generic properties of such a phase transition, which motivates us to study the classical counterpart of the model at finite temperatures.

2. Model and symmetries

In this paper we study a Hamiltonian which is given in terms of spins $\vec{S}_i$ by

$$H = J \sum_{\langle i,j\rangle} \left(2\vec{e}_{i;\langle i,j\rangle} \cdot \vec{S}_i\right) \left(2\vec{e}_{j;\langle i,j\rangle} \cdot \vec{S}_j\right). \tag{1}$$

The sum runs over the bonds of nearest neighbours $\langle i, j\rangle$ of a triangular lattice with N sites. For each bond, only certain projections of the spins $\vec{S}_i$ on unit vectors $\vec{e}_{i;\langle i,j\rangle}$ enter the interaction. These directions are sketched in figure 1. Note that these directions depend on both the bond $\langle i, j\rangle$ and the corresponding end i or j such that three different projections of each spin $\vec{S}_i$ enter the interaction with its six nearest neighbours.

In the derivation from the trimerized kagome lattice [5, 7, 15], the $\vec{S}_i$ are pseudo-spin operators acting on the two chiralities on each triangle and should therefore be considered as quantum spin-1/2 operators. Here we will treat the $\vec{S}_i$ as classical unit vectors. Since only the x- and y-components enter the Hamiltonian (1), one may take the $\vec{S}_i$ as 'planar' two-component vectors. On the other hand, in the quantum case commutation relations dictate the presence of the z-component as well, such that taking the $\vec{S}_i$ as 'spherical' three-component vectors is another natural choice [14]. Here we will compare both choices and thus assess qualitatively the effect of omitting the z-components.

The internal symmetries of the Hamiltonian (1) constitute the dihedral group D_6, i.e. the symmetry group of a regular hexagon. Some of its elements consist of a simultaneous

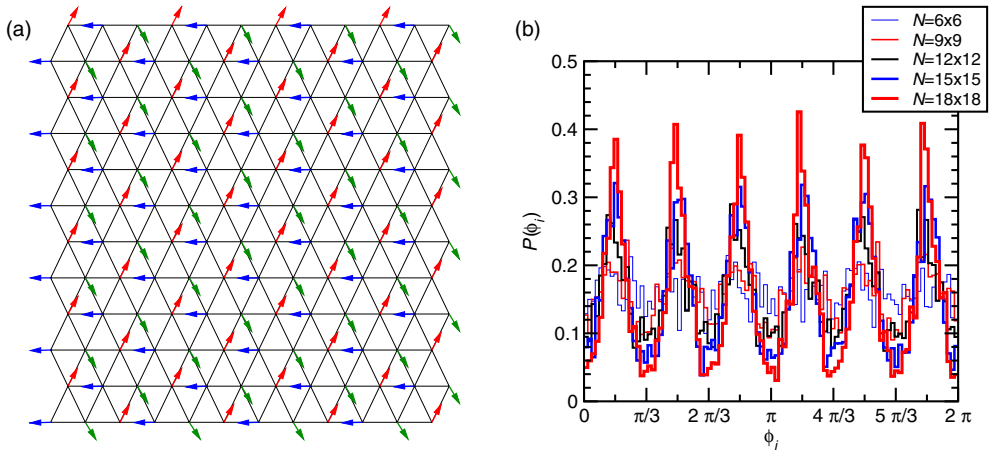

Figure 2. MC results for $J < 0$, $T = 10^{-3}\,|J|$ and planar spins. (a) Snapshot of a configuration on a 12×12 lattice. Periodic boundary conditions are imposed at the edges. (b) Histogram of angles ϕ_i, averaged over 1000 configurations.

transformation of the spins $\vec{S}_i$ and the lattice [14]. Since these symmetries are only discrete, a finite-temperature phase transition is allowed above an ordered groundstate.

The derivation from a spin model [5, 15] yields a positive $J > 0$, while it may also be possible to realize $J < 0$ [8] in a Fermi gas in an optical lattice [7]. In the following we will first discuss the case of a negative exchange constant $J < 0$ and then turn to the case of a positive exchange constant $J > 0$. The second case is more interesting, but also turns out to be more difficult to handle.

3. Negative exchange constant

For $J < 0$ there is a one-parameter family of ordered groundstates, $\vec{S}_i = (\cos(\phi_i), \sin(\phi_i), 0)$, with $\phi_a = \theta$, $\phi_b = \theta + 2\pi/3$ and $\phi_c = \theta - 2\pi/3$ on the three sublattices a, b and c, respectively (120° Néel order). The energy of these states, $E^{J<0} = 6JN$, is independent of θ. Computing the free energy $\mathcal{F}^{J<0}(\theta)$ by including the effect of Gaussian fluctuations we find that $\mathcal{F}^{J<0}(\theta)$ has minima at $\theta = (2n+1)\,\pi/6$, $n = 0,\ 1, \ldots,\ 5$ [14]. This implies that the above 120° Néel structures lock in at these angles.

We have performed Monte Carlo (MC) simulations for $J < 0$ using a standard single-spin flip Metropolis algorithm [16]. A snapshot of a low-temperature configuration on an $N = 12 \times 12$ lattice is shown in figure 2(a). The 120° ordering is clearly seen in such snapshots. Figure 2(b) shows histograms of the angles ϕ_i. One observes that with increasing lattice size N, pronounced maxima emerge in the probability $P(\phi_i)$ to observe an angle ϕ_i at the predicted lock-in values $\theta = (2\,n + 1)\,\pi/6$.

Thermodynamic quantities have been computed by averaging over at least 100 independent MC simulations. Each simulation was started at high temperatures and slowly cooled to lower temperatures in order to minimize equilibration times. A first quantity, namely the specific heat C, is shown in figure 3. There is a maximum in C at $T \approx 1.8\,|J|$ for spherical spins, and for planar spins at a higher temperature $T \approx 2.2\,|J|$. The fact that the value of C around the maximum increases with N indicates a phase transition. For $T \to 0$, the equipartition theorem predicts a contribution $1/2$ to the specific heat per transverse degree of freedom. Indeed, the

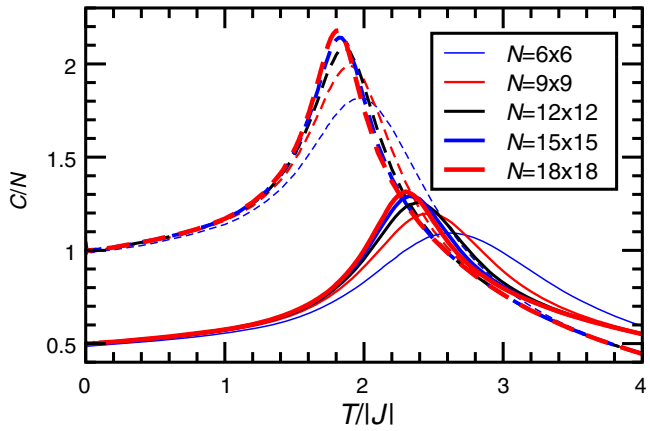

Figure 3. MC results for the specific heat C for $J < 0$. Full lines are for planar spins and dashed lines for spherical spins. Increasing line widths denote increasing system sizes N. Error bars are negligible on the scale of the figure.

low-temperature results are very close to $C/N = 1/2$ and 1 for planar and spherical spins, respectively.

In order to quantify the expected order, we introduce the sublattice order parameter

$$\vec{M}_{\rm s} = \frac{3}{N} \sum_{i \in \mathcal{L}} \vec{S}_i, \tag{2}$$

where the sum runs over one of the three sublattices $\mathcal{L}$ of the triangular lattice. Figure 4 plots the square of this sublattice order parameter

$$m_{\rm s}^2 = \left\langle \vec{M}_{\rm s}^2 \right\rangle, \tag{3}$$

which is a scalar quantity and expected to be non-zero in a three-sublattice ordered state. Note, however, that the order parameter (2) is insensitive to the mutual orientation of spins on the three sublattices. In figure 4 we observe that $m_{\rm s}^2$ converges to zero with $N \to \infty$ at high temperatures, while a non-zero value persists at lower temperatures, consistent with a phase transition around $T \approx 2\,|J|$, as already indicated by the specific heat. Furthermore, the sublattice order again points to a higher transition temperature for planar spins than for spherical spins. It should also be noted that there are noticeable quantitative differences between the values of $m_{\rm s}^2$ for planar and spherical spins over the entire temperature range. Just for $T \to 0$ both planar and spherical spins yield $m_{\rm s}^2 \to 1$, as expected for a perfectly ordered groundstate.

In order to determine the transition temperature $T_{\rm c}$ more accurately, we use the 'Binder cumulant' [16, 17] associated with the order parameter (2) via

$$U_4 = 1 + A - A \frac{\left\langle \vec{M}_{\rm s}^4 \right\rangle}{\left\langle \vec{M}_{\rm s}^2 \right\rangle^2} \qquad \text{with} \quad A = \begin{cases} 1 & \text{for planar spins,} \\ \frac{3}{2} & \text{for spherical spins.} \end{cases} \tag{4}$$

The constants in (4) are chosen such that $U_4 = 0$ for a Gaussian distribution of the order parameter $P(\vec{M}_{\rm s}) \propto \exp(-c\vec{M}_{\rm s}^2)$. Such a distribution is expected at high temperatures, leading to $U_4 \to 0$ for $T \gg |J|$. Conversely, a perfectly ordered state yields $\langle \vec{M}_{\rm s}^4 \rangle = \langle \vec{M}_{\rm s}^2 \rangle^2$ such that with the prefactors as in (4) we find $U_4 = 1$. Hence, for an ordered state we expect $U_4 \approx 1$ for $T < T_{\rm c}$.

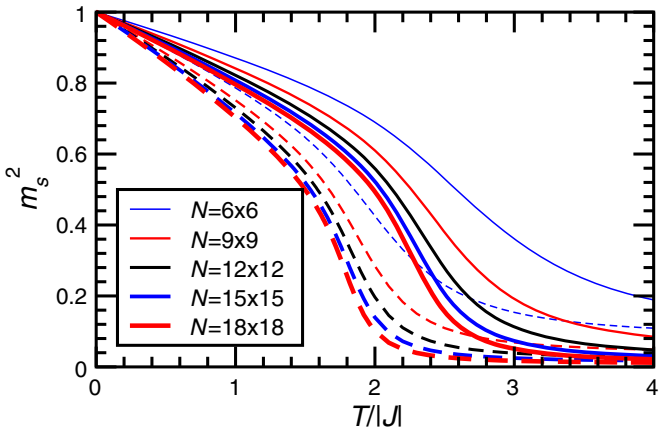

Figure 4. MC results for the square of the sublattice magnetization m_s^2 for $J < 0$. Full lines are for planar spins and dashed lines for spherical spins. Increasing line widths denote increasing N. Error bars are negligible on the scale of the figure.

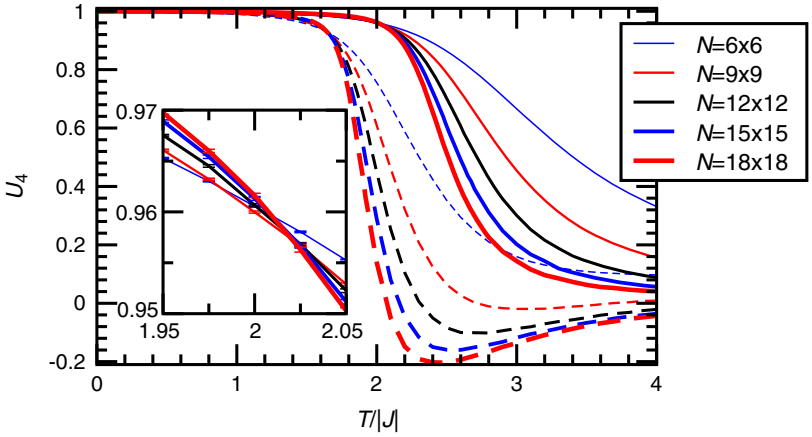

Figure 5. Main panel: MC results for the Binder cumulant for $J < 0$. Full lines are for planar spins; dashed lines for spherical spins. Increasing line widths denote increasing N. Error bars are negligible on the scale of this panel. Inset: Binder cumulant for planar spins close to the critical temperature.

Figure 5 shows our results for the Binder cumulant, as defined in (4). The transition temperature T_c can be estimated from the crossings of the Binder cumulants at different sizes N [16, 17], which are shown for planar spins in the inset of figure 5. Since we have not been aiming at high precision, we cannot perform a finite-size extrapolation. Nevertheless, we obtain a rough estimate

$$T_c^{\text{planar}} \approx 2|J|, \tag{5}$$

with an error on the order of a few per cent. The corresponding value for spherical spins is estimated as $T_c^{\text{spherical}} \approx 1.57\,|J|$ [14]. We therefore conclude that out-of-plane fluctuations reduce T_c by about 20%.

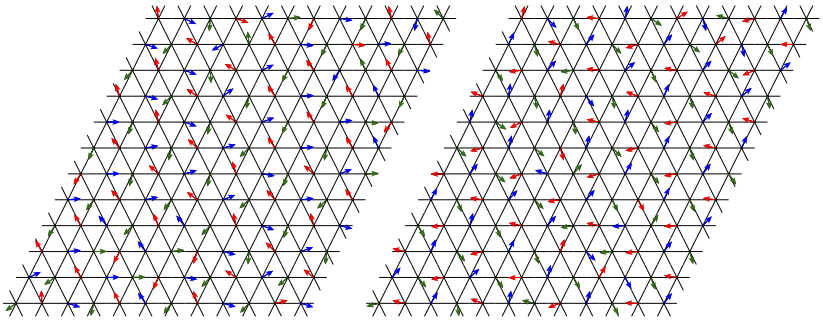

Figure 6. Snapshots of configurations generated by the exchange method at $T \approx 10^{-2}J$ on a 12×12 lattice for planar spins and $J > 0$. Periodic boundary conditions are imposed at the edges.

4. Positive exchange constant

As in the case $J < 0$, there is a one-parameter family of 120° Néel ordered groundstates with energy $-3JN$. They differ from the states found for $J < 0$ by an interchange of the spin directions on the b- and c-sublattices. The contribution of Gaussian fluctuations around these states yields a free energy $\mathcal{F}^{J>0}(\theta)$ which has minima at $\theta = \pi n/3$, $n = 0, 1, \ldots, 5$. Hence the Néel structure locks in at these angles for $J > 0$. Surprisingly, an inspection of all states of finite cells of the lattice, in which the mutual angles between pairs of spins are multiples of $2\pi/3$ [14], reveals that there is a macroscopic number of groundstates in addition to the 120° Néel states, i.e. the number of groundstates grows exponentially with N. The 120° Néel state has $N/3$ soft modes; all other groundstates have fewer soft modes [14]. At low but finite temperatures the 120° Néel state will therefore be selected by a thermal order-by-disorder mechanism [18].

The large number of groundstates which are separated by an energy barrier renders it extremely difficult to thermalize a simple MC simulation at sufficiently low temperatures. We have therefore performed exchange MC simulations (also known as 'parallel tempering') [19, 20] for $J > 0$, using a parallel implementation based on MPI. Ninety-six replicas were distributed over the temperature range $T/J = 0.01, \ldots, 0.7$ in a manner to ensure an acceptance rate for exchange moves of at least 70%. Statistical analysis was performed by binning the time series at each temperature. Figure 6 shows snapshots of two low-temperature configurations with $N = 12 \times 12$ generated by the exchange method with planar spins. In contrast to the case $J < 0$, it is difficult to decide on the basis of such snapshots if any order arises for $J > 0$: there are definitely large fluctuations including domain walls in the system. These fluctuations are in fact a necessary ingredient of the order-by-disorder mechanism. A careful quantitative analysis is therefore clearly needed.

We start with the specific heat C, shown in figure 7. There is a broad maximum at $T \approx 0.25J$ for planar spins and $T \approx 0.3J$ for spherical spins (see figure 7(a)). However, this maximum does not correspond to a phase transition, as one can infer from the small finite-size effects. There is a second small peak in C at a lower temperature $T \approx 0.02J$ (see panels (b) and (c) of figure 7). Since this peak increases with N, it is consistent with a phase transition. Note that at the lowest temperatures C/N is clearly smaller than $1/2$ and 1 for planar and spherical spins, respectively. Indeed, in-plane fluctuations around the 120° state yield one branch of soft modes, which we expect to contribute only $N/12$ to C rather than $N/6$, as the other two branches. Thus, we expect $C/N = 5/12 = 0.416\,66\ldots$ for planar spins and $C/N = 11/12 = 0.916\,66\ldots$ for spherical spins in the limit $T \to 0$. Our MC results

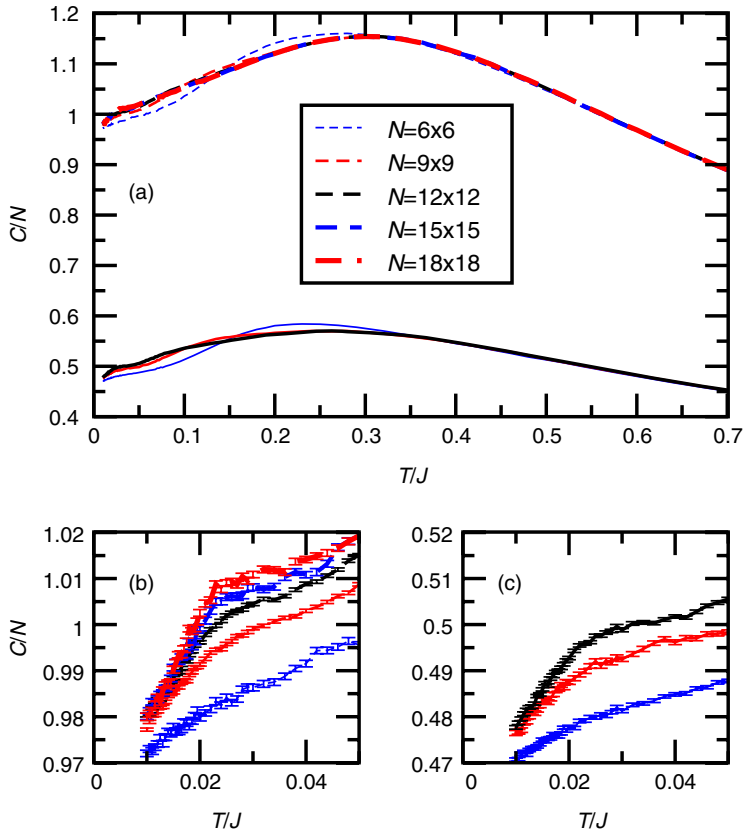

Figure 7. Exchange MC results for the specific heat C for $J > 0$. (a) Full lines are for planar spins; dashed lines for spherical spins. Increasing line widths denote increasing system sizes N. Error bars are of the order of the width of the lines in this panel. The other panels show the low-temperature parts of the results for spherical spins (b), and planar spins (c). The system sizes in panels (b) and (c) range from $N = 6 \times 6$ (bottom) to $N = 18 \times 18$ (panel (b), top), and $N = 12 \times 12$ (panel (c), top), respectively.

tend in this direction, but we have not reached sufficiently low temperatures to fully verify this prediction. Lastly, we note that the difference between C/N for planar and spherical spins is consistent with $1/2$ within error bars only for $T \lesssim 0.02J$.

Next, in figure 8 we show the square of the sublattice magnetization (3) for $J > 0$. First, we observe that it remains small for almost all temperatures and shoots up just at the left side of figure 8 where we measure a maximal value of $m_s^2 \approx 0.4$ for $T = J/100$ on the $N = 6 \times 6$ lattice. This is consistent with a phase transition into a three-sublattice ordered state in the vicinity of the low-temperature peak in the specific heat C. In marked difference with the case $J < 0$ (see figure 4), here we observe only small differences between planar and spherical spins (at least for the sizes where we have data for planar spins, i.e. $N = 6 \times 6$, 9×9 and 12×12).

Finally, figure 9 shows our results for the Binder cumulant, as defined in (4). In contrast to the sublattice magnetization m_s^2, the Binder cumulants for planar and spherical spins are close to each other only for $T \lesssim 0.1J$, provided we scale to the same prefactor A in the definition (4). Again, our best estimate for the transition temperature T_c is obtained from the crossings of the Binder cumulants at different sizes N shown for planar spins in panel (b) of figure 9. The only meaningful crossings are those of the $N = 6 \times 6$ with the $N = 9 \times 9$ and 12×12 curves,

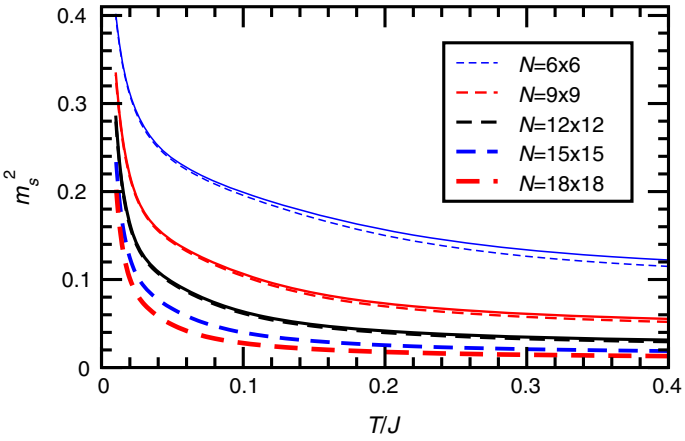

Figure 8. Exchange MC results for the square of the sublattice magnetization m_s^2 for $J > 0$. Full lines are for planar spins; dashed lines for spherical spins. Increasing line widths denote increasing N. Error bars are negligible on the scale of the figure.

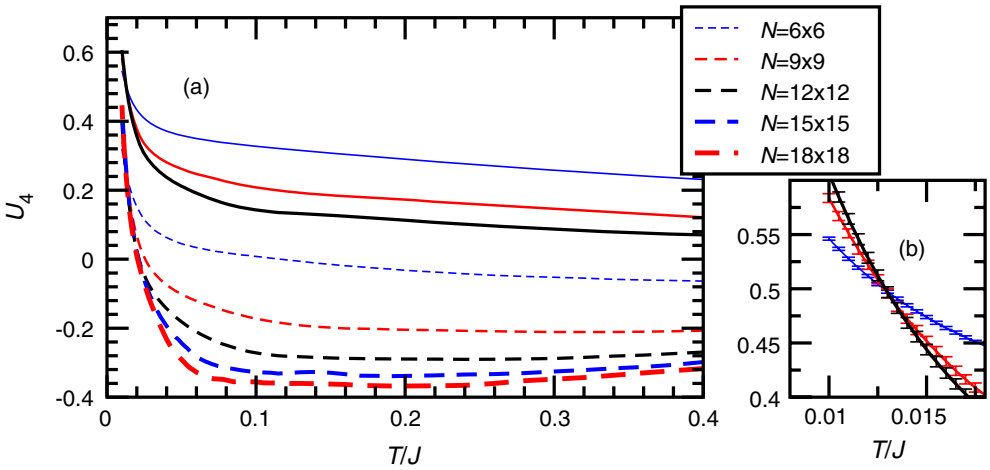

Figure 9. Exchange MC results for the Binder cumulant for $J > 0$. (a) Full lines are for planar spins and dashed lines for spherical spins. Increasing line widths denote increasing N. Error bars are at most of the order of the width of the lines. (b) Binder cumulant for planar spins close to the critical temperature (6). Lines of increasing slope are for increasing system sizes $N = 6 \times 6, 9 \times 9$, and 12×12.

respectively. This leads to a rough estimate

$$T_c^{\text{planar}} \approx 0.0125J. \tag{6}$$

This estimate is indistinguishable from the corresponding value for spherical spins [14], as is expected since the spins lie essentially all in the x–y-plane for such low temperatures.

5. Conclusions and outlook

In this paper we have investigated finite-temperature properties of the classical version of the Hamiltonian (1) on a triangular lattice.

For $J < 0$, we have clear evidence for a low-temperature phase with 120° Néel order. The transition temperature is of order $|J|$ and can be determined with reasonable accuracy. Planar and spherical spins yield qualitatively similar results, but there are quantitative differences, in particular the transition temperature (5) is higher for planar spins. We have performed further simulations for spherical spins [14] in order to determine critical properties. On the one hand, so far we have no evidence for a discontinuity at T_c, on the other hand the assumption of a continuous phase transition yields very unusual critical exponents [14] which violate the hyperscaling relation. Thus, the most plausible scenario may be a weakly first-order transition.

For $J > 0$, the groundstates are macroscopically degenerate [14]. A thermal order-by-disorder mechanism [18] predicts the selection of another 120° ordered state. The corresponding phase transition is just at the limits of detectability even with the exchange MC method [19, 20]: we find an extremely low transition temperature (6) which is two orders of magnitude smaller than the overall energy scale J. In this case, the spins lie essentially in the x–y-plane in the relevant temperature region such that we obtain quantitatively extremely close results for planar and spherical spins in the vicinity of T_c, apart from a constant offset in the specific heat.

The features observed for example in the specific heat for the classical variant resemble those found in the original quantum model [12–14]. Since only much smaller systems are numerically accessible for the quantum model, the results for the classical variant are an important tool for understanding the quantum case. In particular, the finite-temperature phase transitions should be universal and may therefore be characterized in the classical model. However, highly accurate data are needed for that purpose. Our result that spherical and planar spins exhibit the same qualitative features for $J < 0$, and that for $J > 0$ the z-component is even quantitatively very small in the relevant temperature range, may be useful in this context. Namely, one may choose planar spins for further simulations, thus reducing the number of degrees of freedom to be updated.

Acknowledgments

Useful discussions with F Mila are gratefully acknowledged. We are indebted to the CECPV, ULP Strasbourg for allocation of CPU time on an Itanium 2 cluster. This work has been supported in part by the European Science Foundation through the Highly Frustrated Magnetism network. Presentation at HFM2006 is supported by the Deutsche Forschungsgemeinschaft through SFB 602.

References

[1] Schollwöck U, Richter J, Farnell D J J and Bishop R F 2004 *Quantum Magnetism* (*Springer Lecture Notes in Physics* vol 645) (Berlin: Springer)
[2] Diep H T 2005 *Frustrated Spin Systems* (Singapore: World Scientific)
[3] Lecheminant P, Bernu B, Lhuillier C, Pierre L and Sindzingre P 1997 *Phys. Rev.* B **56** 2521
[4] Waldtmann Ch, Everts H-U, Bernu B, Lhuillier C, Sindzingre P, Lecheminant P and Pierre L 1998 *Eur. Phys. J.* B **2** 501
[5] Subrahmanyam V 1995 *Phys. Rev.* B **52** 1133
[6] Mila F 1998 *Phys. Rev. Lett.* **81** 2356
Mambrini M and Mila F 2000 *Eur. Phys. J.* B **17** 651
[7] Santos L, Baranov M A, Cirac J I, Everts H-U, Fehrmann H and Lewenstein M 2004 *Phys. Rev. Lett.* **93** 030601
[8] Fehrmann H 2006 Strongly correlated systems in ultracold quantum gases *PhD Thesis* Universität Hannover
[9] Cabra D C, Grynberg M D, Holdsworth P C W, Honecker A, Pujol P, Richter J, Schmalfuß D and Schulenburg J 2005 *Phys. Rev.* B **71** 144420
[10] Nussinov Z and Fradkin E 2005 *Phys. Rev.* B **71** 195120

[11] Dorier J, Becca F and Mila F 2005 *Phys. Rev.* B **72** 024448
[12] Damski B, Everts H-U, Honecker A, Fehrmann H, Santos L and Lewenstein M 2005 *Phys. Rev. Lett.* **95** 060403
[13] Damski B, Fehrmann H, Everts H-U, Baranov M, Santos L and Lewenstein M 2005 *Phys. Rev.* A **72** 053612
[14] Cabra D C, Everts H-U, Honecker A, Pujol P and Stauffer F 2006 in preparation
[15] Zhitomirsky M E 2005 *Phys. Rev.* B **71** 214413
[16] Landau D P and Binder K 2000 *A Guide to Monte Carlo Simulations in Statistical Physics* (Cambridge: Cambridge University Press)
[17] Binder K 1981 *Z. Phys.* B **43** 119
[18] Villain J, Bidaux R, Carton J-P and Conte R 1980 *J. Physique* **41** 1263
Shender E F and Holdsworth P C W 1996 *in Fluctuations and Order: A New Synthesis* ed M M Millonas (Berlin: Springer)
[19] Hukushima K and Nemoto K 1996 *J. Phys. Soc. Japan* **65** 1604
[20] Marinari E 1998 *in Springer Lecture Notes in Physics* vol 501 (Berlin: Springer) (cond-mat/9612010)